

# Fractal Hexagonal Disc Shaped Ultra Wideband Antenna

A.M.M.Allam<sup>1</sup>, M. H. Abdelazeem<sup>2</sup>

<sup>1</sup>German University in Cairo,  
Cairo, Egypt

<sup>2</sup>AAST, Cairo, Egypt

**Abstract-**

In this paper, we have investigated printed monopole antennas with different radiating patch configurations on defected ground plane or UWB applications. Traditional circular disc patch, hexagonal patch, and first and second Koch iterations of fractal hexagonal patch are presented. The traditional disc is operating along the frequency band from 2.6 GHz to 10.9 GHz, while the hexagonal patch is operating from 2.6 GHz to 10.7GHz. On the other hand first and second Koch iterations are operating over 2.5 GHz to 13.5GHz. The antennas are printed on Rogers RO4350 substrate of thickness 1.5245mm with relative permittivity 3.66 and dielectric loss tangent 0.004. The printed antennas are supported by a concentric hexagonal notch patch on the back of the radiating patch. Some of the proposed antennas are fabricated and experimentally investigated. There is a good agreement between the measured return loss and the simulated one. The antenna gives symmetrical omnidirectional patterns.

**Keywords** -Ultra wideband (UWB) antenna; Disc antenna; Hexagonal antenna; Fractal antenna; Printed monopole antenna.

**1. Introduction**

Wireless communication has developed significantly over the recent two decades [1]. This tremendous growth of the wireless communication, with the ever increasing amount of wireless devices, will cause future innovations to face spectral crowding. Furthermore, conjunction of wireless devices will have a chance to be a significant issue. Therefore, the Ultra Wideband (UWB) devices are needed as they operate at various large frequency bands. Recently [2] UWB antenna plays an important role in communication system due to its low cost, low power consumption, low interference, capability of high data rate of around 100 megabits/second.

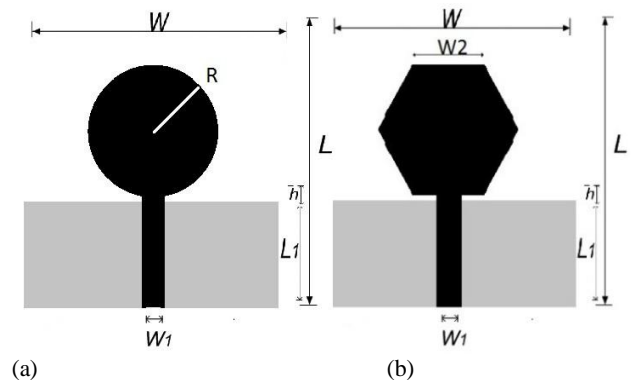
UWB technology has a data transfer capacity wider over

500 MHz alternately a 20% fractional bandwidth. Federal Communication Commission (FCC) allowed the use of unlicensed bandwidth from 3.1 GHz to 10.6 GHz [3]. The technique to increase the bandwidth (BW) of circular antenna might have been suggested toward Kraus on 1988 [4] by tapering the connection between feed line and the antenna.

Also fractal geometry play an important role in fabricating antennas with more bandwidth and smaller dimension compared to conventional antennas [5]. Fractals make starting with self-similar elements, which would iterate to different directions. Moreover, their states do not transform by expanding iterations [6]. Available fractal geometries for wideband applications are Sierpinski, Koch, Minkowski, and Pythagorean tree [7-10]. In this article Koch fractal iteration is adopted

**2. Antenna design and geometry**

The proposed antennas are depicted in Fig.1. The radiating patch is etched on the top layer and depicted in black color while, the defected ground in the back layer is illustrated with gray color. The antennas are printed on Rogers RO4350 substrate of thickness 1.5245mm with relative permittivity 3.66 and dielectric loss tangent 0.004. All antennas are fed by a 50 microstrip line of width  $W_1$  and length  $L_1+h$ .



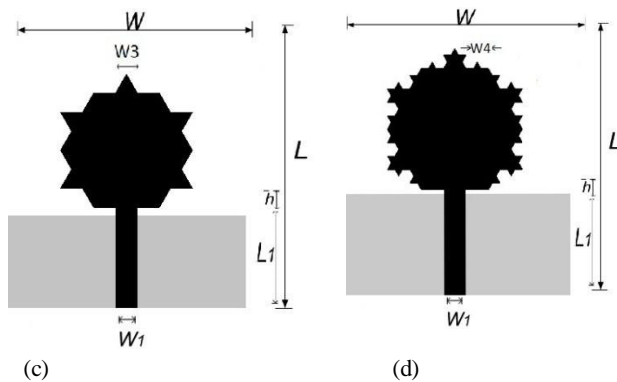


Fig.1 Printed Monopole Antennas  
 (a) Traditional Disc (b) Hexagonal Patch  
 (c) Koch 1<sup>st</sup> Iteration (d) Koch 2<sup>nd</sup> iteration

The overall substrate dimensions of each antenna is  $W \times L$ ;  $50 \times 42 \text{ mm}^2$  where  $W$  is the substrate width and  $L$  is the length of the substrate. The other dimensions are illustrated in table 1 where,  $L_1$  is the ground length (grey colored),  $h$  is the gap between the patch and the ground,  $W_2$  is the length of the hexagonal side,  $W_3$  is the length of the first iteration equilateral triangle side and  $W_4$  is the length of the second iteration equilateral triangle side. The hexagonal patch on Fig.1b has been designed to reach as much as possible the same area of the traditional disc on Fig.1a. The first and second iterations patches on Fig.1c, and Fig.1d are formed by applying Koch fractal curve defined in Eq. (1) & Eq. (2) [11], where  $N_k$  is the number of sides,  $L_k$  is the length of a side at any given degree of iteration ( $k$ ) and  $x$  is the side length of each of the three sides of the original triangle as shown in Fig.2

$$N_k = (3)4^k \quad (2)$$

$$(1) L_k = (x)3^{-k}$$

Fig.2 Koch Iterated Curves

The dimensions of the different four antennas are depicted in table1.

Parameter (mm)	Traditional Disc	Hexagonal	1 <sup>st</sup> iteration	2 <sup>nd</sup> iteration
R	10.5			
h	0.2	0.788	0.788	0.788
W1	3.363	3.363	3.363	3.363
L1	16.8	16.8	16.8	16.8
W2		11.55	11.55	11.55
W3			3.85	3.85
W4				1.283
Area(mm <sup>2</sup> )	346.36	346.589	378.35	392.46

Fig.3 shows the fabricated monopole printed antennas of traditional disc, hexagonal patch and Koch first iteration hexagonal patch.

### 3. Simulated and measured results

The characteristics of the proposed antennas have been analyzed by CST Microwave Studio software. Fig.4 shows the simulated results for return loss of the antennas (traditional disc, hexagonal, first and second iterations). For the traditional disc the lowest frequency is 2.6 GHz and highest frequency is 10.9 GHz achieving 8.3 GHz bandwidth with fractional bandwidth of 122.9%, the hexagonal patch operates along the frequency range from 2.6 GHz to 10.7 GHz with bandwidth 8.1 GHz and 121.8% fractional bandwidth, while the first and the second iterations operate along the frequency range from 2.5GHz to 13.5 GHz achieving 11GHz with fractional bandwidth 137.5%.



Fig.3 Fabricated Monopole Antennas

Fig.5, Fig.6 and Fig.7 illustrate the simulated versus measured return loss for traditional disc, hexagonal patch and the Koch first iteration hexagonal patch respectively. The measured and simulated results are in agreement to a great extent.

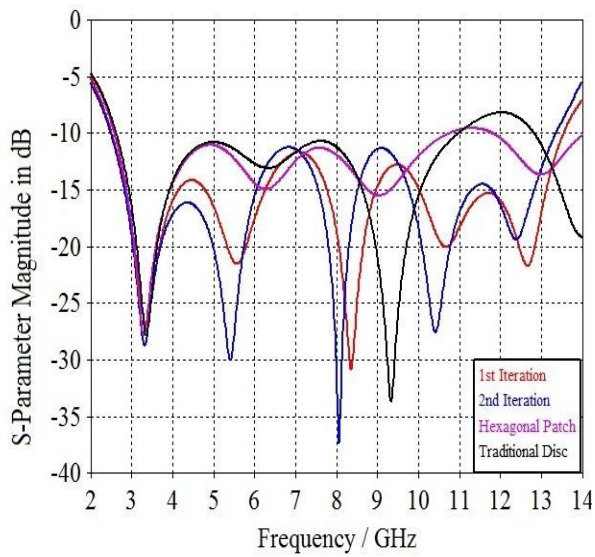


Fig.4 Return Loss of Simulated Monopole Antennas

It is important to point out that when applying fractal Koch first and second iterations the bandwidth increases by about 25%

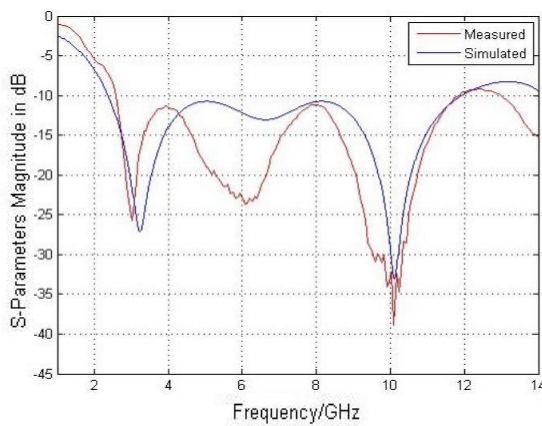


Fig.5 Traditional Disc Return Loss

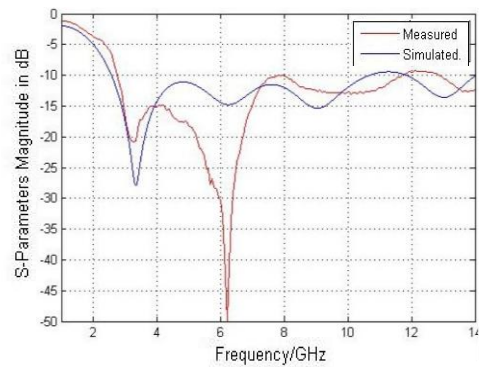


Fig.6 Hexagonal Patch Return Loss

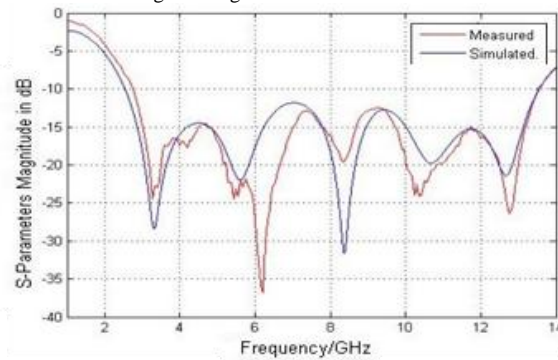


Fig.7 First Iteration Return

The radiation pattern of the Koch first iteration hexagonal patch monopole is selected and depicted in Fig.8 for different frequencies in both E and H planes. The antenna average gain is 5.8 dB.

Fig.9 shows the current distributions along the printed first Koch iteration hexagonal patch monopole at different frequencies. It is clear that the current is surrounding the edges and microstrip feed. Fig.10 illustrates the simulated group delays of the four antennas along the operating band. It is clear that the group delays are within the range which is convenient for digital communications.

(b)

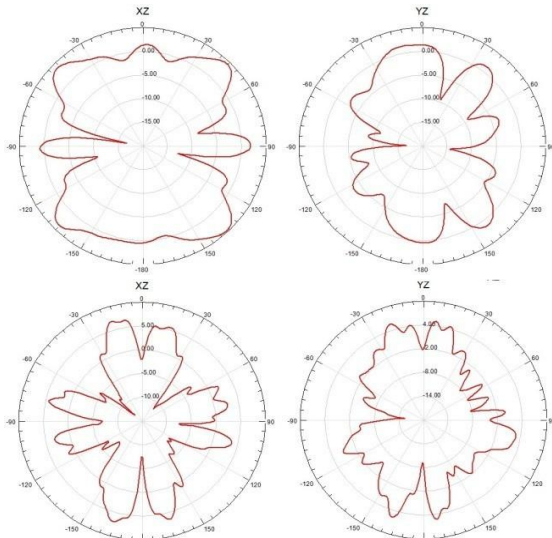


Fig.8 Radiation Patterns in E and H Planes  
(a) f=4GHz (b) f=13GHz

Fig.12 illustrates simulated return loss for the case of Koch first iteration radiating patch at different notch patch side lengths. On the other hand, table 2 and 3 summarize the simulated notch frequency  $f_0$  and associated bandwidths for all radiating patch at different side length  $W_f$ . Table 2 concerns the traditional and hexagonal radiating patch while table 3 depicts the results for Koch first and second iteration radiating patches.

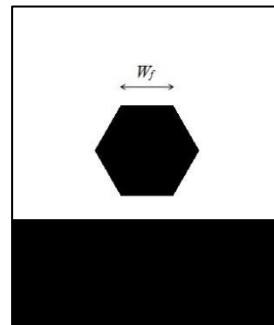


Fig.11 Hexagonal Patch Notch on the Back

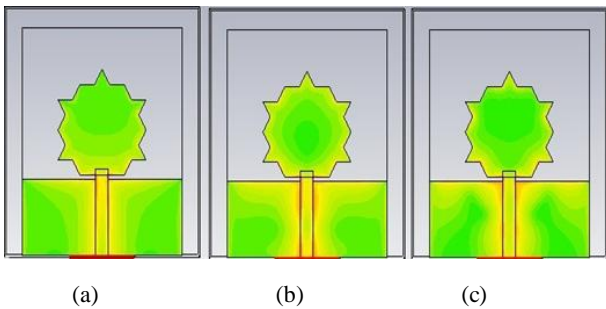


Fig.9 Surface Current Distribution at Different Frequencies  
(a) At 3GHz (b) At 7GHz (c) At 11GHz

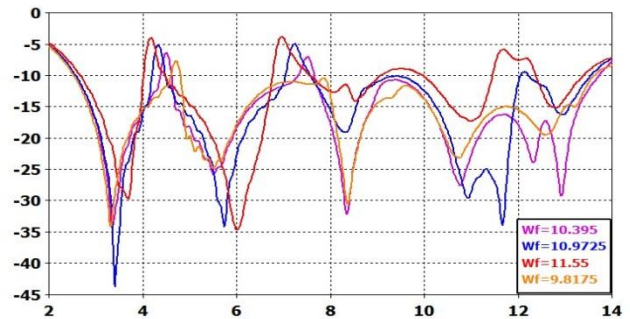


Fig.12 Return Loss of 1<sup>st</sup> Iteration Patch with Different Hexagonal Notch Pch Side Lengths

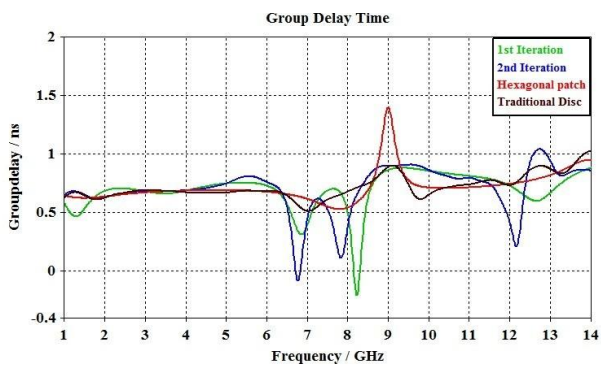


Fig.10 Group Delay of Different Antenna Configurations

Moreover, the printed antennas are supported by a concentric hexagonal notch patch on the back of the radiating patch as shown in Fig.11. This notch patch conducts different notch frequencies according to its side length  $W_f$  and the chosen radiating patch.

Table 2 Simulated Notch Frequencies for Hexagonal Notch Patch

$W_f$	Radiating Patch			
	Traditional Disc		Hexagonal Patch	
	$f_o$ (MHz)	BW (MHz)	$f_o$ (MHz)	BW (MHz)
<b>8.6625</b>	5075	550	5130	460
<b>9.24</b>	4855	510	4850	500
	8355	390	8350	500
<b>9.8175</b>	4695	430	4650	500
	8030	560	7985	570
	10750	300		
<b>10.395</b>	4615	490	4555	290
	7810	760	7705	610
	10650	500		
<b>10.9725</b>	4555	710	4400	340
	7635	970	7705	730
	10525	750		
<b>11.55</b>	4590	1120	4555	1110
	7465	1310	7545	1410
	10150	760		

Table 3 Simulated Notch Frequencies for Hexagonal Notch Patch

$W_f$	Radiating Patch			
	1 <sup>st</sup> Iteration		2 <sup>nd</sup> Iteration	
	$f_o$ (MHz)	BW (MHz)	$f_o$ (MHz)	BW (MHz)
<b>8.6625</b>				
<b>9.24</b>	4935	130		
<b>9.8175</b>	4695	210	4680	160
<b>10.395</b>	4495	250	4475	210
	7465	370	7385	270
<b>10.9725</b>	4330	300	4295	250
	7300	540	7090	460
	12130	180	9050	720
<b>11.55</b>	4400	480	4120	440
	7155	810	7020	720
	9515	910	8925	1350
	11910	940	11720	700

## 4. Conclusion

Four printed monopole antennas are presented for UWB applications. Traditional disc patch, hexagonal patch, and the first and second Koch iterations of fractal hexagonal patch are investigated as radiating patches. They conduct frequency bands 2.6GHz-10.9GHz, 2.6GHz-10.7GHz, 2.5GHz-13.5GHz respectively. A hexagonal notch patch is introduced on the back of the radiating patch, where its side length is used for tuning the antennas to remove the band required. There is a good agreement between the measured return loss and the simulated one. The antennas give symmetrical omnidirectional patterns.

## References

- [1] Huseyin Arslan, Zhi Ning Chen, Maria\_Gabriella Di Benedetto, "Ultra wideband wireless communication", John Wiley & sons, 2006.
- [2] R. Garg, P. Bhartia, I. Bahl and A. Ittipiboon "Microstrip antenna design handbook", Artech House, Norwood, MA, USA, 2001.
- [3] M.Ghavami, L.B. Michael, R.Kohno, "Ultra wideband Signals and Systems in Communication Engineering", 2nd Edition, John Wiley & sons, 2007.
- [4] Kraus, J. D., Antennas, 2nd Edition, 692-694, McGraw Hill, New York, 1988.
- [5] Azari, A. and J. Rowhani, "Ultra wideband fractal microstrip antenna design," Progress In Electromagnetics Research C, Vol. 2, 7-12, 2008.
- [6] Cohen, N., "Fractal antenna options for wideband and beyond wireless," Calgary, 2003.
- [7] D. H. Werner and S. Ganguly, "An overview of fractal antenna engineering research," IEEE Antennas and Propagation Magazine, vol. 45, no. 1, pp. 38-57, 2003.
- [8] B. Manimegalai, S. Raju, and V. Abhaikumar, "A multifractal Cantor antenna for multiband wireless applications," IEEE Antennas and Wireless Propagation Letters, vol. 8, pp. 359-362, 2009.
- [9] J. Pourahmadazar, C. Ghobadi, J. Nourinia, and H. Shirzad, "Multiband ring fractal monopole antenna for mobile devices," IEEE Antennas and Wireless Propagation Letters, vol. 9, pp. 863-866, 2010.
- [10] M. Naghshvarian-Jahromi, "Novel wideband planar fractal monopole antenna," IEEE Transactions on Antennas and Propagation, vol. 56, no. 12, pp. 3844-3849, 2008.
- [11] J. Feder, "Fractals," Plenum, New York, 1988